An image reconstruction method from Fourier data with uncertainties on the spatial frequencies

2013 J. Phys.: Conf. Ser. 464 012008

(http://iopscience.iop.org/1742-6596/464/1/012008)

Journal of Physics: Conference Series **464** (2013) 012008 doi:10.1088/1742-6596/464/1/012008

An image reconstruction method from Fourier data with uncertainties on the spatial frequencies

Anastasia Cornelio[1], Silvia Bonettini[2] and Marco Prato[1]

[1] Dipartimento di Scienze Fisiche, Informatiche e Matematiche, Università di Modena e Reggio Emilia, Via Campi 213/b, 41125 Modena, Italy
[2] Dipartimento di Matematica e Informatica, Università di Ferrara, Via Saragat 1, 44122 Ferrara, Italy

E-mail: marco.prato@unimore.it

Abstract. In this paper the reconstruction of a two-dimensional image from a nonuniform sampling of its Fourier transform is considered, in the presence of uncertainties on the frequencies corresponding to the measured data. The problem therefore becomes a blind deconvolution, in which the unknowns are both the image to be reconstructed and the exact frequencies. The availability of information on the image and the frequencies allows to reformulate the problem as a constrained minimization of the least squares functional. A regularized solution of this optimization problem is achieved by early stopping an alternating minimization scheme. In particular, a gradient projection method is employed at each step to compute an inexact solution of the minimization subproblems. The resulting algorithm is applied on some numerical examples arising in a real-world astronomical application.

1. Introduction

Fourier imaging finds applications in several scientific and medical areas, as computerized tomography, magnetic resonance imaging and astronomy [4, 9]. More in general, a Fourier approach is adopted when the high frequencies characterizing the measured radiation make the acquisition systems designed for optical wavelengths unsuitable. In this paper, we address the Fourier image reconstruction problem in which the frequencies corresponding to the data samples are not exactly known, but some estimates of them are available. Problems in which the degraded image has to be found without prior knowledge of the system PSF are typically known as blind deconvolution [17, 18, 19]. In particular, in our case we are dealing with a semi-blind deconvolution problem [2, 10, 11], since the PSF is not completely unknown but a parametrized version is available. Due to the usual non-negativity of the image and the partial a priori information on the frequencies, the reconstruction problem can be reformulated as a constrained nonlinear least squares problem. We propose to address its solution by means of a cyclic block gradient projection scheme, in which at each cycle either the image or the parametrized PSF is kept fixed, while the other is updated through a certain number of gradient projection iterations. Moreover, a suitable criterion allows us to perform only few cycles, thus leading to a regularized solution thanks to the semiconvergent behaviour of a general iterative approach. The proposed scheme is then validated with some numerical tests on simulated datasets, designed within a real-world astronomical application.

2. Imaging from Fourier data

The Fourier imaging problem aims at reconstructing a n^2-vector f, representing the discretization of an unknown non-negative distribution $f(x, y)$ (rearranged in lexicographic order), starting from the knowledge of an N-vector g containing the corresponding measured or estimated complex Fourier samples. Mathematically, this can be done by solving the minimization problem

$$\min_{f\in\mathbb{R}^{n^2},\ f\geq 0} \Phi(f) \equiv \frac{1}{2}\|Af - g\|^2_{\mathbb{C}^N}, \tag{1}$$

where the $N \times n^2$ matrix A is defined as

$$(A)_{hk} = e^{2\pi i \rho_k (x_h \cos(\theta_k) + y_h \sin(\theta_k))}, \quad h = 1, \ldots, n^2, \quad k = 1, \ldots, N. \tag{2}$$

Here (θ_k, ρ_k) are the spatial frequencies corresponding to the sample g_k, given in polar coordinates (in several applications, like the one described in Section 3, the data acquisition system makes a polar representation of the spatial frequency more convenient than the classical Cartesian one).

If the data frequencies are not completely known, but only some ranges of variability are available, then problem (1) becomes

$$\min_{\substack{f\in\mathbb{R}^{n^2},\ f\geq 0\\ \theta\in\mathbb{R}^N,\ \theta^{\min}\leq\theta\leq\theta^{\max}\\ \rho\in\mathbb{R}^N,\ \rho^{\min}\leq\rho\leq\rho^{\max}}} \Phi(f, \theta, \rho) \equiv \frac{1}{2}\|A(\theta, \rho)f - g\|^2_{\mathbb{C}^N}, \tag{3}$$

where $\theta = (\theta_1, ..., \theta_N)^T$ and $\rho = (\rho_1, ..., \rho_N)^T$ are the vectors of angular and radial coordinates, and $\theta^{\min}$, $\theta^{\max}$, $\rho^{\min}$, $\rho^{\max}$ are the related lower and upper bounds.

Problem (3) is convex if restricted to f only, but is nonconvex with respect to θ and ρ and, even more, with respect to (f, θ, ρ), thus leading to the possible presence of several local minima.

Due to the separate nature of the optimization variables, we approached the minimization problem (3) by means of an alternating strategy [13, 14], consisting in the following iterative minimization scheme:

$$f^{(\ell+1)} = \operatorname*{argmin}_{f\geq 0} \Phi(f, \theta^{(\ell)}, \rho^{(\ell)}) \tag{4}$$

$$\theta^{(\ell+1)} = \operatorname*{argmin}_{\theta^{\min}\leq\theta\leq\theta^{\max}} \Phi(f^{(\ell+1)}, \theta, \rho^{(\ell)}) \tag{5}$$

$$\rho^{(\ell+1)} = \operatorname*{argmin}_{\rho^{\min}\leq\rho\leq\rho^{\max}} \Phi(f^{(\ell+1)}, \theta^{(\ell+1)}, \rho) \tag{6}$$

The key problem is that the proposed scheme has two nontrivial drawbacks, since a) the convergence to a solution of (3) is not guaranteed (see e.g. the counterexample shown by Powell in [25]), and b) computing the exact minimum points in each subproblem is impractical. Both problems can be avoided by solving inexactly each partial minimization problem by means of a suitable descent method [5, 13]. In particular, this occurs when the approximation of each solution of (4)–(6) is achieved by performing a finite number of iterations of the gradient projection (GP) method [7], that applies to any minimization problem over a convex set Ω of the form

$$\min_{x\in\Omega} \psi(x)$$

and whose main steps are reported in Algorithm 1.

The GP method and its scaled version SGP [7] combine a gradient projection step with variable steplength (and scaling) with the well-known Armijo rule to achieve the sufficient decrease in the

Algorithm 1 Gradient projection method

Choose the starting point $x^{(0)} \in \Omega$, set the parameters $\nu, \mu \in (0,1)$, $0 < \alpha_{min} < \alpha_{max}$.

FOR $k = 0, 1, 2, \ldots$ DO THE FOLLOWING STEPS:

STEP 1. Choose the steplength parameter $\alpha_k \in [\alpha_{min}, \alpha_{max}]$;
STEP 2. Projection: $y^{(k)} = P_\Omega(x^{(k)} - \alpha_k \nabla\psi(x^{(k)}))$;
STEP 3. Descent direction: $\Delta x^{(k)} = y^{(k)} - x^{(k)}$;
STEP 4. Backtracking loop: set $\lambda_k = 1$.
IF $\psi(x^{(k)} + \lambda_k \Delta x^{(k)}) \leq \psi(x^{(k)} + \nu\lambda_k \nabla\psi(x^{(k)})^T \Delta x^{(k)}$ THEN go to Step 5;
ELSE set $\lambda_k = \mu\lambda_k$ and go to Step 4.
ENDIF
STEP 5. Set $x^{(k+1)} = x^{(k)} + \lambda_k \Delta x^{(k)}$.

END

Algorithm 2 Cyclic block gradient projection method

Choose $f^{(0)} \geq 0$, $\theta^{\min} \leq \theta^{(0)} \leq \theta^{\max}$, $\rho^{\min} \leq \rho^{(0)} \leq \rho^{\max}$ and three integers $N_f, N_\theta, N_\rho \geq 1$.

FOR $\ell = 0, 1, 2, \ldots$ DO THE FOLLOWING STEPS:

STEP f. Choose an integer $1 \leq N_f^{(\ell)} \leq N_f$ and compute $f^{(\ell+1)}$ by applying $N_f^{(\ell)}$ iterations of Algorithm 1 to problem (4) starting from the point $f^{(\ell)}$.
STEP θ. Choose an integer $1 \leq N_\theta^{(\ell)} \leq N_\theta$ and compute $\theta^{(\ell+1)}$ by applying $N_\theta^{(\ell)}$ iterations of Algorithm 1 to problem (5) starting from the point $\theta^{(\ell)}$.
STEP ρ. Choose an integer $1 \leq N_\rho^{(\ell)} \leq N_\rho$ and compute $\rho^{(\ell+1)}$ by applying $N_\rho^{(\ell)}$ iterations of Algorithm 1 to problem (6) starting from the point $\rho^{(\ell)}$.

END

objective function [3]. As concerns the choice of the steplength parameter, notable results have been obtained in denoising and deblurring problems [21, 26] by alternating the two Barzilai-Borwein rules [1, 12]. More details on GP and its parameters can be found e.g. in [6, 24].
In conclusion, problem (3) can be approximately solved by applying to the minimum problems (4)–(6) a finite number of GP steps: the resulting scheme is the cyclic block gradient projection (CBGP) method detailed in Algorithm 2 and any limit point of the sequence $(f^{(\ell)}, \theta^{(\ell)}, \rho^{(\ell)})$ is stationary (see [5, Theorem 4.2]).

3. An application in astronomy

In this section we test the proposed scheme in a real-world application in astronomy, namely the reconstruction of X-ray images of a solar flare. The Fourier samples of the unknown image are estimated from a set of count profiles provided by the solar satellite RHESSI [20], launched by NASA on February 5 2002 to study solar flares and other energetic solar phenomena. Due to the RHESSI imaging hardware, based on rotating modulation collimator techniques [15], the data frequencies are arranged around nine concentric circles in the Fourier plane whose radii form a geometric sequence with a common ratio $\sqrt{3}$ (see Figure 1). In particular, the total number of data N is given by the sum of the N_i samples on each circle ($i = 1, \ldots, 9$).
The resulting mathematical model is given by

$$\min_{\substack{f \in \mathbb{R}^{n^2},\ f \geq 0 \\ \theta \in \mathbb{R}^N,\ \theta^{\min} \leq \theta \leq \theta^{\max}}} \Phi(f, \theta) \equiv \frac{1}{2} \|A(\theta) f - g\|^2_{\mathbb{C}^N}, \tag{7}$$

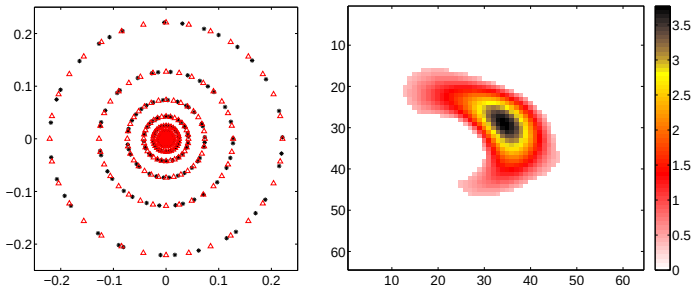

Figure 1. *Left panel*: example of distribution of the sampling points for the RHESSI imaging problem (black asterisks), together with the bounds of the box constraints $\theta^{\min}, \theta^{\max}$ (red triangles). *Right panel*: image of a real flare used as ground truth for the simulated datasets.

that is a particular case of (3) in which the radial coordinate ρ of each sample is known. The CBGP approach is compared with the Space-D algorithm [6], that is a GP method developed within the RHESSI data analysis framework for solving the minimum problem (1). As all the other Fourier-based reconstruction algorithms designed for RHESSI [8, 22], Space-D assumes that, for the i-th circle ($i = 1, \ldots, 9$), the angular coordinate θ is given by the middle points of a uniform partition of the $[0, 2\pi]$ range in N_i bins, since in most cases this choice provides a good estimate of the real value. Our CBGP approach allows to remove this assumption, and to treat the value of θ as a further unknown of the reconstruction problem, using the uniform discretization to define the box constraints (see Figure 1).

We generated a simulated dataset by selecting an image of a real flare (April 15 2002, 00:05:00–00:10:00 UT, energy band 12-14 keV - see Figure 1, right panel) and calculating the corresponding data through numerical integration of the Fourier Transform. As concerns the choice of θ, we chose a random angle within each box $[\theta^{\min}, \theta^{\max}]$. The Fourier samples in this dataset will be characterized by the presence of a systematic source of noise only, due to the fact that in the inversion procedure the exact value of θ is unknown. We refer to this dataset with the term "Sim". Finally, we corrupted the resulting data by realistic statistical noise (estimated by assuming Poisson noise on the original count profiles), and this last dataset will be denoted by "Sim_N". We point out that our way to generate the simulated dataset is a very simplified version of the much more sophisticated procedure employed by RHESSI. We chose this procedure since it allows to know the "true" values of θ and, therefore, to evaluate the effectiveness of the blind approach. In particular, the choice of angles θ according to a uniform random distribution is arbitrary.

As for the CBGP parameters, we used the same values selected for the Space-D algorithm: in particular, the stopping criterion chosen to terminate the iterations in both steps of the cyclic approach[1] is given by

$$|\psi(x^{(k)}) - \psi(x^{(k-1)})| < 10^{-4}|\psi(x^{(k)})|. \tag{8}$$

The choice of the threshold 10^{-4} guarantees a limited number of iterations at each step and, therefore, a regularization effect on the recovered solution (more details are shown in [7]). The CBGP scheme is initialized with a vector $\theta^{(0)}$ equal to the middle points of each bin. In these settings, the image reconstructed by the Space-D algorithm is exactly $f^{(1)}$ (see Algorithm 2). As far as the number of cycles ℓ concerns, the CBGP algorithm is stopped when criterion (8) in either the step on f or the step on θ is satisfied at the first iteration (in addition, a maximum number of cycles equal to 20 is imposed).

[1] We remark that in this situation both the block–iterative optimization methods described in Section 2 reduce to the alternate inexact solution of subproblems (4)–(5).

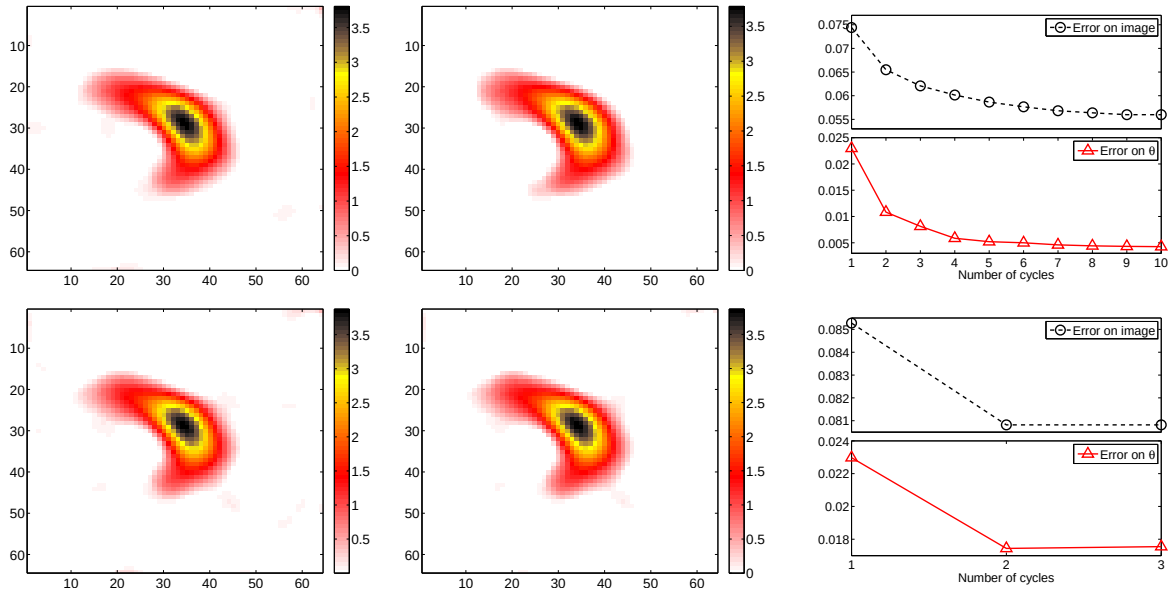

Figure 2. Results of the simulated tests Sim (top row) and Sim_N (bottom row). The images obtained with Space-D (first column) and CBGP (second column) are presented, together with the reconstruction errors on the image and, for CBGP, on the angular coordinates (third column).

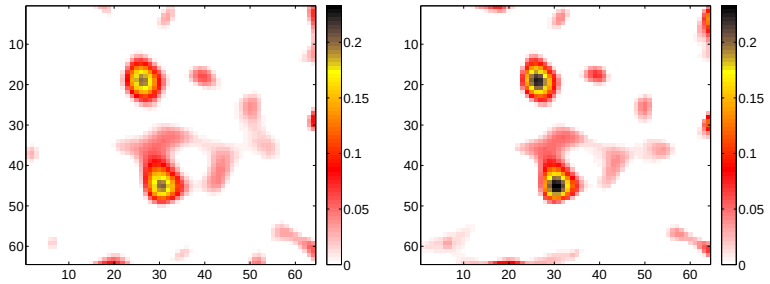

Figure 3. Reconstructions obtained from real data with Space-D (left panel) and CBGP (right panel).

In Figure 2 we report the reconstructed images obtained with Space-D (first column) and CBGP (second column), together with the relative errors in Euclidean norm on both the image and the angular coordinates (third column), for the Sim (top row) and Sim_N datasets (bottom row). As remarked before, the reconstruction error provided by Space-D is the one obtained at the first cycle. From the results obtained we can see that the blind approach is able to improve the image quality with respect to the Space-D algorithm, thanks to a better estimate of the underlying array θ. Although the restored images appear to be very similar, some details are better reconstructed, as the right footpoint of the loop in the Sim case. The lower number of cycles performed in the noisy case is in agreement with the fact that, in presence of statistical noise, the effect of a bad choice for θ is more negligible (even if still present). We remark that, for the considered application, the computational time is not a crucial issue, since both Space-D and CBGP end in few seconds.
Fore sake of completeness, we also considered a real event occurred on February 20, 2002 (11:06:02–11:06:34 UT, energy band 22-26 keV) and we show the reconstructions obtained with Space-D and CBGP in Figure 3.

4. Conclusions and future work

In this work we considered the image reconstruction problem from a sampling of its Fourier Transform, in the specific case in which only estimates of the frequencies corresponding to the measured data are available. From the mathematical point of view, the presence of uncertainties on the frequencies can be translated in a constrained least-squares problem, in which the matrix that describes the link between data and image is not known a priori, but depends on a vector of parameters to be determined. The natural subdivision of the unknowns in separate groups led us to choose a cyclic block alternating method for the resolution of the optimization problem. In particular, we used a strategy in which each subproblem is solved inexactly by means of a projected gradient method, which on the one hand provides a convergent scheme, and on the other hand allows us to avoid the (onerous) exact resolution of each subproblem. As numerical experiments, we chose to test the method on a simulated dataset inspired by a real application in astronomy, and the results seem to validate the proposed scheme.
Future work will involve the extension of the semi-blind approach to objective functions including regularization penalties on the image, like the Tikhonov term for smooth objects or an edge-preserving function for sharp contents. As regards the astronomical application considered in this work, we would like to extend the proposed methodology to the reconstruction of electrons images through the Bremsstrahlung integral equation [16, 23].

Acknowledgements

This work has been partially supported by the FIRB - Futuro in Ricerca research project "Apprendere nel tempo: un nuovo approccio computazionale per l'apprendimento automatico di sistemi dinamici", contract RBFR12M3AC_002, and the research project "Metodi numerici e software per l'ottimizzazione su larga scala con applicazioni all'image processing" of the Italian Gruppo Nazionale per il Calcolo Scientifico (GNCS-INdAM).

References

[1] Barzilai J and Borwein J M 1988 *IMA J. Numer. Anal.* **8** 141–8
[2] Benvenuto F and Ferrari A 2010 *Inverse Probl.* **26** 105011
[3] Bertsekas D P 1999 *Nonlinear programming* (Belmont, MA: Athena Scientific)
[4] Blahut R E 2001 *Theory of Remote Image Formation* (Cambridge: Cambridge University Press)
[5] Bonettini S 2011 *IMA J. Numer. Anal.* **37** 1431–52
[6] Bonettini S and Prato M 2010 *Inverse Probl.* **26** 095001
[7] Bonettini S Zanella R and Zanni L 2009 *Inverse Probl.* **25** 015002
[8] Bong S C Lee J Gary D E and Yun H S 2006 *Astrophys. J.* **636** 1159–65
[9] Bracewell R 2000 *The Fourier Transform and its applications* (New York, NY: McGraw-Hill)
[10] Conan J M Mugnier L M Fusco T Michau V and Rousset G 1998 *Appl. Opt.* **37** 4614–22
[11] Christou J C Bonnacini D Ageorges N and Marchis F 1999 *Messenger* **97** 14–22
[12] Frassoldati G Zanni L and Zanghirati G 2008 *J. Indust. Manag. Optim.* **4** 299–312
[13] Grippo L and Sciandrone M 1999 *Optim. Method Softw.* **10** 587–637
[14] Grippo L and Sciandrone M 2000 *Oper. Res. Lett.* **26** 127–36
[15] Hurford G J et al 2002 *Solar Phys.* **210** 61–86
[16] Kontar E P et al 2011 *Space Sci. Rev.* **159** 301–55
[17] Kundur D and Hatzinakos D 1996 *IEEE Signal Proc. Mag.* **13**(3) 43–64
[18] Kundur D and Hatzinakos D 1996 *IEEE Signal Proc. Mag.* **13**(6) 61–63
[19] Levin A Weiss Y Durand F and Freeman W T 2009 *IEEE Conf. Computer Vision and Pattern Recognition* pp 1964–71
[20] Lin R P et al 2002 *Solar Phys.* **210** 3–32
[21] Loris I Bertero M De Mol C Zanella R and Zanni L 2009 *Appl. Computat. Harmon. A.* **27** 247–54
[22] Massone A M et al 2009 *Astrophys. J.* **703** 2004–16
[23] Prato M 2009 *Arch. Comput. Method E.* **16** 109–60
[24] Prato M Cavicchioli R Zanni L Boccacci P and Bertero M 2012 *Astron. Astrophys.* **539** A133
[25] Powell M J D 1973 *Math. Program.* **4** 193–201
[26] Zanella R Boccacci P Zanni L and Bertero M 2009 *Inverse Probl.* **25** 045010